Layered $[BaM(C_3H_2O_4)_2(H_2O)_4]$ (M = Fe or Co) Complexes − Spectroscopic, Magnetic and Thermal Study

Izaskun Gil de Muro,[a] Luis Lezama,[a] Maite Insausti,[a] and Teófilo Rojo*[a]

Keywords: Magnetic properties / Barium / Iron / Cobalt / Thermochemistry

Complexes with formula $[BaM(C_3H_2O_4)_2(H_2O)_4]$, where M = Fe or Co, were synthesised and characterised. These two types of complexes are isostructural and crystallise in the *Pccn* space group. Their structure consists of two-dimensional networks of octahedral MO_6 polyhedra in which the transition metal ions are coordinated by bridging malonate ligands, through the O-C-O atoms. These M-malonate units are extended along the crystallographic [101] plane. Spectroscopic data are consistent with the cations being in a high-spin octahedral symmetry. The two types of compounds exhibit 2D antiferromagnetic interactions as well as weak ferromagnetism below the Néel temperature, as a result of an intralayer misalignment of the spins. Thermal treatment of the metallo-organic precursors gave rise to $BaMO_{3-y}$ oxides at lower temperatures and reaction times than those found in the literature using the ceramic method.

Introduction

The chemistry of heteronuclear complexes involving bridging carboxylate ligands has been exhaustively investigated using a wide variety of physical techniques such as electronic spectroscopy, susceptibility measurements, EPR spectroscopy,... with the aim of understanding the structural and chemical factors that govern the exchange coupling between paramagnetic centres.

The malonate ligand, with two neighbouring carboxylate groups, is a very flexible ligand which can adopt a monodentate mode, various bischelating coordination modes and different carboxylate bridging modes (*syn-syn, syn-anti,* and *anti-anti*).[1] It is a useful tool for connecting different metal ions and transmitting different magnetic interactions. In this way, ferromagnetically[2] or antiferromagnetically[3] coupled dimers, alternating chains,[4,5] polymeric trinuclear antiferromagnetic complexes[6,7] and two-dimensional ferromagnetic and antiferromagnetic compounds[8,9] have been obtained and studied.

On the other hand, these complexes can be used as an alternative to the ceramic method in the synthesis of mixed oxides.[10,11] In this sense, several studies with different metallo-organic precursors, employing carboxylate ligands such as edta,[12] oxalate[13] and tartrate,[14] or nitrite[15] have been carried out, and more recently using the malonate ligand.[8,16−18]

Malonate complexes such as $[AM(C_3H_2O_4)_2(H_2O)_4]$, where A is Sr or Ba and M is Mn or Cu, showed interesting spectroscopic and magnetic properties. Furthermore, their usefulness as precursors of mixed oxides was proved, and homogeneous oxides with small particles were obtained by thermal treatment of $[AM(C_3H_2O_4)_2(H_2O)_4]$.[8] In this paper we describe the synthesis and the spectroscopic and magnetic properties of the $[BaM(C_3H_2O_4)_2(H_2O)_4]$ (M = Fe or Co) compounds, together with their thermal study. These complexes will be abbreviated as BaFe and BaCo.

Results and Discussion

Crystallographic Study

Powder X-ray diffraction patterns of the microcrystalline products were recorded. Indexation of the diffraction profile and refinement of the cell parameters were made by FULLPROF (pattern-matching analysis)[19] on the basis of the space group *Pccn* and the cell parameters found for a single crystal of $[SrCu(C_3H_2O_4)_2(H_2O)_4]$, as published previously[8] (see Figure 1). The obtained crystallographic data for the $[BaM(C_3H_2O_4)_2(H_2O)_4]$ (M = Fe or Co) complexes are given in Table 1. The variation of the cell volume is in good agreement with the corresponding cation size. Taking these results into account, we have considered the two phases to be isostructural to the already characterised phase SrCu.[8] The structure consists of two-dimensional networks of transition metal ions coordinated by bridging malonate ligands. These M-malonate units are infinitely extended along the crystallographic [101] plane (see Figure 2). The metallic centres are octahedrally coordinated, with two oxygen atoms from two bidentate malonate anions at basal sites and two oxygen atoms from two malonate anions at apical sites. These bridging arrangements by carboxylate

[a] Dpto. Química Inorgánica, Facultad de Ciencias. UPV/EHU, Apdo. 644, 48080 Bilbao, Spain
Fax: (internat.) +34-94/464-8500
E-mail: qiproapt@lg.ehu.es

  DOI: 10.1002/ejic.200300077

groups form infinite sheets where the shortest M···M distances occur through the O-C-O atoms. The alkaline earth cations are located between the M-malonate layers and are coordinated to four oxygens of different malonates and to two lattice water molecules, forming a distorted antiprism.

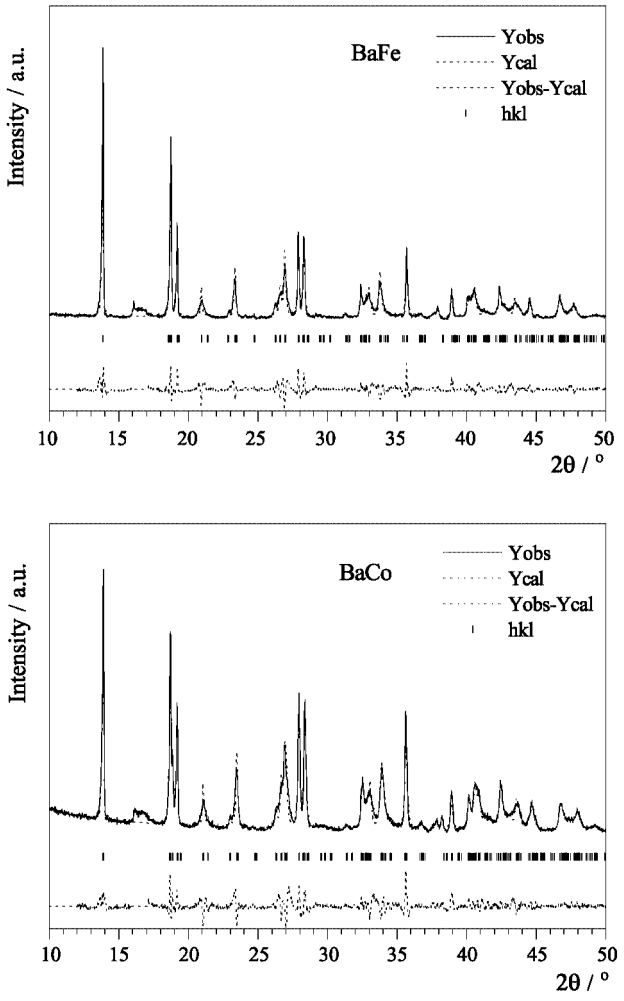

Figure 1. Observed, calculated and difference XRD profiles for the BaFe and BaCo phases

Table 1. Crystallographic data for the $[BaM(C_3H_2O_4)_2(H_2O)_4]$ (M = Fe, Co) compounds

	BaFe	BaCo	SrCu[a]
Molecular mass	469.28	472.36	427.27
Crystal system	Orthorhombic	Orthorhombic	Orthorhombic
Space group	Pccn	Pccn	Pccn
a (Å)	6.795(2)	6.782(1)	6.719(2)
b (Å)	18.948(4)	18.976(3)	18.513(7)
c (Å)	9.492(3)	9.407(2)	9.266(4)
V (Å^3)	1222.1	1210.0	1152.6

[a] Data calculated from a single crystal study.[8]

Thermal Study

The thermal decomposition steps of the compounds were obtained from the TG curves shown in Figure 3. The thermogravimetric data are summarised in Table 2. Decomposition arises from three consecutive processes: dehydration, ligand pyrolysis and inorganic residue formation.

The first process takes places in the 75−100 °C temperature range and corresponds to the loss of four water molecules. This process occurs in only one step, suggesting that all the water molecules are similar. This was also deduced from the crystallographic data of the SrCu compound. No significant differences between the treatments in air and nitrogen atmospheres were observed, except for slight displacements in the decomposition-temperature ranges.

The second stage involves the decarboxylation of the ligand, and takes place in the 250−450 °C temperature range. The following reaction schemes are the most plausible way of describing the decomposition process:$MM'L_2$ (s) → MCO_3 (s) + $M'CO_3$ (s) + R (g) (a)$MM'L_2$ (s) → MO (s) + $M'CO_3$ (s) + R (g) (b)$MM'L_2$ (s) → MO (s) + $M'O$ (s) + R (g) (c)

The main factor controlling the pyrolysis process is the nature of the cation coordinated to the ligand[20] and, depending on the stability of the metal carbonates, reactions *(a)*, *(b)* or *(c)* can occur. In our case, as alkaline-earth metal carbonates are stable, the ligand pyrolysis can be described by the second reaction. The weight loss is in good accordance with the decarboxylation of the malonate ligand to yield $BaCO_3$ and the corresponding transition metal oxide. The oxide obtained can vary depending on the applied atmosphere. Therefore, we propose that the Fe_2O_3 and Co_3O_4 oxides are formed in air while the Fe_2O_3 and CoO oxides are obtained under a nitrogen atmosphere.

Finally, a gradual mass loss is observed at temperatures above 600 °C, when carbonate decomposes and mixed oxides are formed. At this stage, the applied atmosphere plays an important role; either complete decomposition under nitrogen is not reached or more reduced mixed oxides are obtained. In fact the inorganic residues analysed by X-ray diffraction indicated the presence of different $BaFeO_{3-y}$ and $BaCoO_{3-y}$ mixed oxides.

Following this study, and in order to obtain pure phases of mixed oxides, several thermal treatments in tubular furnaces were carried out. After firing the BaFe and BaCo malonate precursors at 400 °C, investigations at higher temperatures and different atmospheres were performed for each case. The resulting products were characterised at each stage by X-ray powder diffraction (see Figure 4). The thermal decomposition of the $[BaFe(C_3H_2O_4)_2(H_2O)_4]$ precursor was carried out under an oxygen atmosphere at 800 °C to yield the non-stoichiometric oxide $BaFeO_{3-y}$.[21] In the case of the barium cobalt metallo-organic precursor, a treatment at 700 °C in air was needed in order to obtain the non-stoichiometric $BaCoO_{3-y}$ as a pure phase.[22]

Spectroscopic Properties

Infrared Spectroscopy

The IR spectra of the $[BaM(C_3H_2O_4)_2(H_2O)_4]$ (M = Fe or Co) compounds are very similar. Broad bands observed

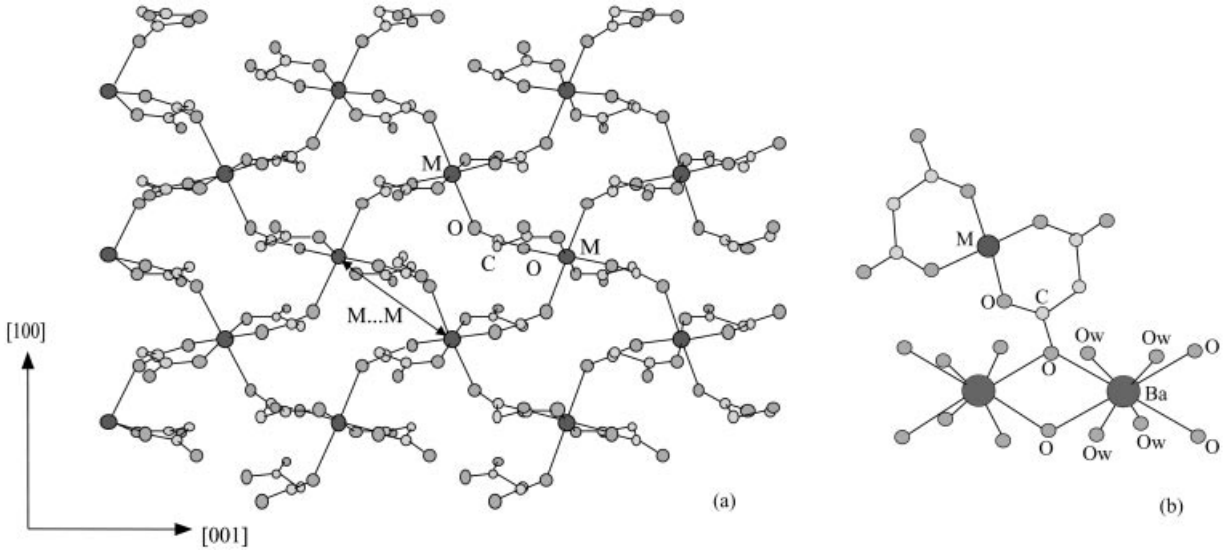

Figure 2. (a) Two-dimensional network of transition metal polyhedra and (b) alkaline earth centre and junction to transition metal polyhedra in $[AM(C_3H_2O_4)_2(H_2O)_4]$

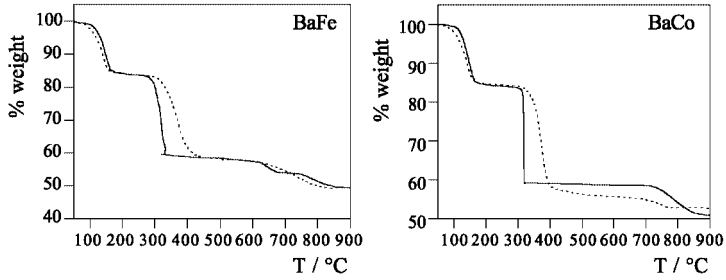

Figure 3. TG curves of the BaFe and BaCo complexes, under air (– –) and nitrogen (···)

Table 2. Thermogravimetric data of the $[BaM(C_3H_2O_4)_2(H_2O)_4]$ (M = Fe, Co) precursors

Stage			*T* (°C)	% weight[a]	Products
Dehydration	BaFe	air	100–180	84.5 (84.4)	$[BaFe(C_3H_2O_4)_2]$
		N_2	70–180	85.0 (84.4)	$[BaFe(C_3H_2O_4)_2]$
	BaCo	air	95–190	85.0 (84.7)	$[BaCo(C_3H_2O_4)_2]$
		N_2	75–175	85.5 (84.7)	$[BaCo(C_3H_2O_4)_2]$
Ligand pyrolysis	BaFe	air	275–340	59.0 (59.1)	$BaCO_3 + Fe_2O_3$
		N_2	290–450	58.8 (59.1)	$BaCO_3 + Fe_2O_3$
	BaCo	air	300–320	59.0 (58.8)	$BaCO_3 + Co_3O_4$
		N_2	310–420	57.0 (57.6)	$BaCO_3 + CoO$
Inorganic residue formation	BaFe	air	600–700, 730-	53.5 (51.4)	$BaFeO_3$
		N_2	635–865	–	$BaCO_3 + Ba_2Fe_2O_5$
	BaCo	air	685-	–	$BaCoO_3$
		N_2	690-	–	$BaCO_3 + Co_2O_3$

[a] Theoretical values in brackets.

in the 3300–3500 cm^{-1} region, can be assigned to the stretching vibration, ν(O-H), of the hydroxyl groups in the water molecules. The next group of bands appearing at around 2900 cm^{-1} corresponds to the stretching vibration, ν(C-H), of the malonate ligands. The band observed at 1730 cm^{-1} for the malonic acid is shifted in the titled compounds to 1600 cm^{-1}. This fact is indicative of the coordination of the carboxylate groups to the metal ions. This band appears together with the antisymmetric $\nu_a(OCO^-)$ vibration, whereas the band corresponding to the symmetric $\nu_s(OCO^-)$ vibration is localised at 1370 cm^{-1}. Taking the relative position of the antisymmetric $\nu_a(OCO^-)$ and symmetric $\nu_s(OCO^-)$ vibration bands into account, we can conclude that the bonding between the metal and the ligand gives rise to a chelate.[23] This observation is supported by the crystal data obtained from the SrCu compound. Finally, the bending vibration corresponding to the δ(C=O) group is observed at around 1300 cm^{-1}.

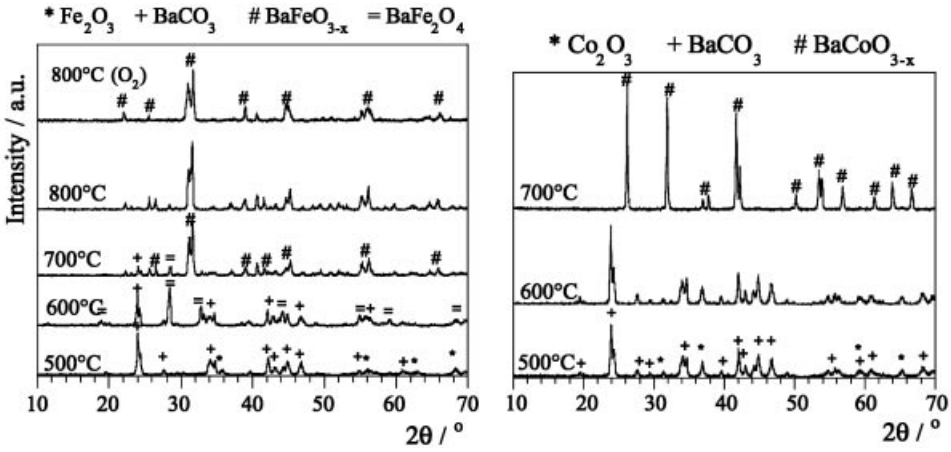

Figure 4. XRD patterns of the phases obtained from the thermal treatment of the BaFe and BaCo precursors

Diffuse Reflectance Spectroscopy

The reflectance spectra of the BaFe and BaCo complexes were recorded at room temperature in the 5000−45000 cm^{-1} range. For the iron phase, a single band appears which corresponds to the ${}^5E_g \leftarrow {}^5T_{2g}$ transition and is characteristic of a high-spin d^6 configuration in octahedral coordination. From the position of this band, the Dq parameter was calculated to be 1150 cm^{-1}, in good agreement with the usual values found for octahedrally coordinated iron(II). The spectrum of the BaCo compound shows three bands: at (ν_1) 8300, (ν_2) 15500 and (ν_3) 20600 cm^{-1}, which were assigned to the following three allowed transitions: ${}^4T_{2g} \leftarrow {}^4T_{1g}\ (F)$, ${}^4A_{2g} \leftarrow {}^4T_{1g}\ (F)$ and ${}^4T_{1g}\ (P) \leftarrow {}^4T_{1g}\ (F)$, respectively. By considering an octahedral model, the values of Dq (940) and B (753 cm^{-1}) were calculated from the ν_1 and ν_3 transitions. These values agree with those obtained for cobalt(II) compounds in an octahedral geometry.[24]

Magnetic Properties

Magnetic susceptibility measurements of powdered samples of $[BaM(C_3H_2O_4)_2(H_2O)_4]$ (where M = Fe or Co) were carried out in the 1.8−300 K temperature range, with applied magnetic fields of 1 and 0.1 kG. The χ_m and $\chi_m T$ vs. T curves of both compounds are shown in Figure 5, together with those of BaMn, given for comparison. All the calculated magnetic data are summarised in Table 3.

The μ_{eff} values measured at room temperature are 5.23 and 4.96 μ_B, for the BaFe and BaCo complexes respectively, and correspond to high-spin states for both metallic cations. In both cases, the $\chi_m T$ data decrease with decreasing temperature, reaching a minimum value at about 15 K. Then, the curves suddenly increase and at lower temperatures decrease again, reaching a maximum in $\chi_m T$ at around 12 K.

The χ_m^{-1} vs. T curves follow Curie−Weiss behaviour above 20 K, the Weiss constant, θ, being negative (−19.33 and −48.94 K), and the Curie constant, C_m, being 3.636 and 3.59 $cm^3 \cdot K \cdot mol^{-1}$ for the iron and cobalt compounds, respectively. The high value of θ found for the cobalt complex can be attributed to the spin-orbit coupling effect.

The initial progressive decrease of the $\chi_m T$ data until 15 K, together with the negative values of θ, are indicative of the presence of antiferromagnetic interactions. Considering the structural features of these compounds, the high-temperature susceptibility data were fitted to a two-dimensional Heisenberg antiferromagnetic model, employing the expansion series given by Rushbrooke and Wood.[25] Equation (1), (2) and (3) were deduced by taking into account the S = 5/2, 2 and 3/2 values for the Mn^{II}, Fe^{II} and Co^{II}, respectively, and are based on the spin Hamiltonian $H = -2J \Sigma_{<i,\ j>} S_i S_j$:

$$\chi_m = 2.91\ (Ng^2\beta^2)/(kT)\ [1 + 23.33x + 147.78x^2 + 405.48x^3 + 8171.3x^4 + 64968x^5 + 15811x^6]^{-1} \quad (1)$$

$$\chi_m = 2.00\ (Ng^2\beta^2)/(kT)\ [1 + 16x + 72x^2 + 195.067x^3 + 1781.87x^4 + 10301.4x^5 + 14736.4x^6]^{-1} \quad (2)$$

$$\chi_m = 1.25\ (Ng^2\beta^2)/(kT)\ [1 + 10x + 30x^2 + 42.6667x^3 + 262.917x^4 + 1043.85x^5 + 790.112x^6]^{-1} \quad (3)$$

where $x = J/kT$.

The BaMn susceptibility data gave the following values: g = 1.99 and J/k = −0.59 K,[8] indicating the presence of weak antiferromagnetic interactions. The best fit found for the iron and cobalt complexes is represented by the corresponding continuous lines in Figure 5. In the case of BaFe, the experimental data agree with values of g = 2.187 and J/k = −0.95 K only up to 30 K. At lower temperatures the curve clearly deviates from the theoretical model. As the maximum in χ_m is out of the fitting range, the calculated J value should be considered as a simple approximation. In this case, the zero-field splitting effect should be taken into account, especially at low temperatures. For the cobalt compound, the calculated J/k and g values are −3.24 K and 2.679, respectively, even though the inaccuracy of the model is obvious. The spin-orbit coupling effect progressively changes from a spin state S = 3/2 in the octahedral cobalt(II) ion to an effective spin state S' = 1/2 at low temperatures. Nevertheless, we can assume that until 15 K the

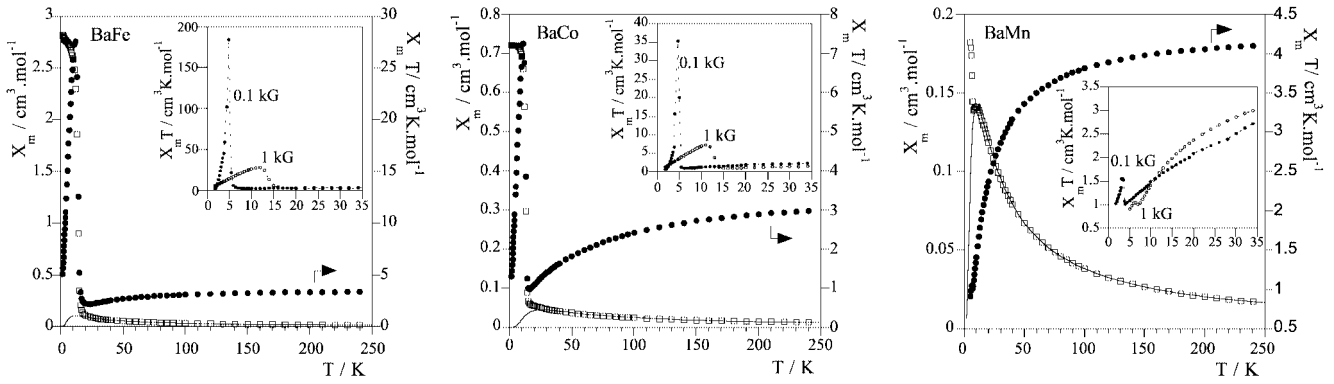

Figure 5. Thermal evolution of χ_m and $\chi_m T$ for BaFe, BaCo and BaMn, measured at 1 kG. (The $\chi_m T$ vs. T curves measured at 0.1 *k*G are represented in the insets)

Table 3. Magnetic parameters of the BaFe, BaCo and BaMn compounds

		T_N/K	C_m/cm^3·K·mol^{-1}	θ /K	μ $_{eff}$/μ_B
BaFe	AF + weak FM	13.2	3.64	−19.3	5.23
BaCo	AF + weak FM	13	3.59	−48.9	4.96
BaMn[8]	AF + weak FM	7	4.34	−13.8	5.76

three compounds show two-dimensional Heisenberg antiferromagnetic behaviour with a weak intralayer antiferromagnetic interactions between the $M^{II}\cdots M^{II}$ atoms through the O-C-O bridges. Below 15 K, the presence of the minimum in the $\chi_m T$ curve together with a sudden increase indicates that total antiparallel alignment of the spins is not reached, suggesting the presence of long-range magnetic ordering due to the existence of interlayer ferromagnetic coupling. Moreover, this is a field-dependent effect: the less intense is the applied field (0.1 kG), the sharper is the maximum observed (see insets in Figure 5). In both cases, the field dependency is more intense than that observed for the BaMn compound.

In order to study this effect, magnetization measurements were performed. The results are shown in Figure 6. The magnetization shows a linear dependence on the magnetic field at 20 K. However, at 5 K both curves became nonlinear, indicating the presence of a ferromagnetic component at this temperature. For the BaFe compound, an anomalous dependence is also observed, probably due to the zero-field splitting effect (see Figure 6a).

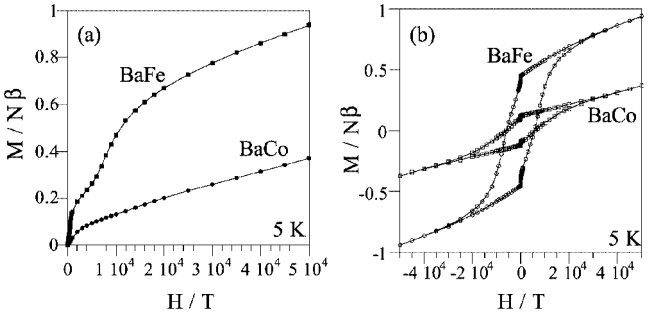

Figure 6. (a) M vs. H and (b) hysteresis curves at 5 K for the BaFe and BaCo compounds

The hysteresis curves M vs. H measured at 5 K are also indicative of the presence of ferromagnetic interactions. Both compounds show small hysteresis loops, with coercive fields of 6000 G, and remnant magnetization values of 0.44 and 0.12 in $N\beta$ units for the iron and cobalt complexes, respectively (see Figure 6b).

Finally, the thermoremnant magnetization was measured at a magnetic field of 100 G. The M_r vs. T curves are shown in Figure 7. The Néel temperatures are 13.2 K and 13 K for BaFe and BaCo, respectively. Both curves show a rapid increase reaching saturation with thermoremnant magnetization values of 0.44 and 0.12 in $N\beta$ units for the BaFe and BaCo compounds, respectively. These values agree with the M_r ones found in the hysteresis loops, and corroborate the existence of weak ferromagnetism in both samples. For BaMn, complete ordering was not reached even at 4 K (see inset in Figure 7), the ferromagnetic component in this compound being weaker than in BaFe and BaCo. Following these results, we must assume that the magnitude of the

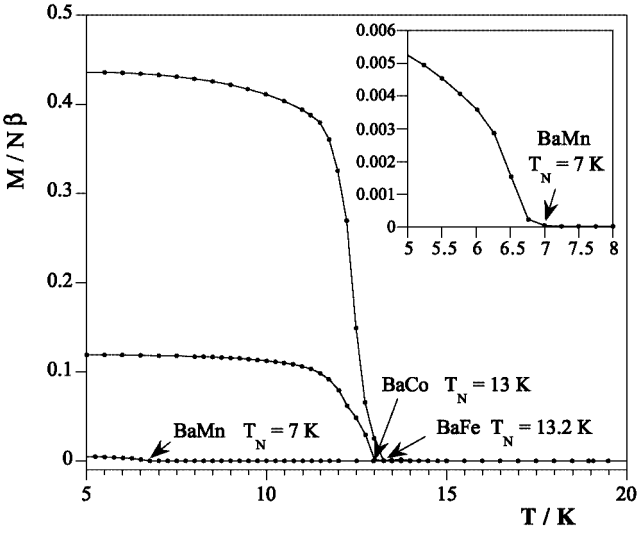

Figure 7. Zero-field magnetization vs. T curves for the BaFe, BaCo and BaMn compounds, after cooling, under a magnetic field of 100 G

ferromagnetic component cannot depend only on the spin value of the metallic cation. Other parameters such as magnetic anisotropy of the cations, exchange angles and bond lengths should be considered in order to explain the magnetic behaviour observed in these compounds. Notwithstanding, and taking all the results into account, we can conclude that the BaMn, BaFe and BaCo compounds show 2D Heisenberg antiferromagnetic behaviour above 15 K, as a result of an intralayer antiferromagnetic interaction between M···M atoms, through the O-C-O bridges. Below this temperature, the total coupling of the antiparallel spins is not reached, probably due to the existence of an intralayer misalignment of the spins (or canting)[8] and a long-range ferromagnetic ordering between layers, with a weak ferromagnetism being observed.

Conclusions

Two new two-dimensional compounds, $[BaFe(C_3H_2O_4)_2(H_2O)_4]$ and $[BaCo(C_3H_2O_4)_2(H_2O)_4]$, have been synthesised. They are isostructural with the $[SrCu(C_3H_2O_4)_2(H_2O)_4]$ phase. These complexes exhibit two-dimensional antiferromagnetic interactions and below 12 K the presence of weak ferromagnetism has also been detected. This observation was attributed to the presence of long-range magnetic ordering of the canted spins between layers.

The thermal decomposition of the compounds occurs in three steps: dehydration, pyrolysis of the ligand and evolution of the inorganic residue to yield mixed oxides. Different thermal treatments in tubular furnaces at temperatures between 700−850 °C and under different atmospheres gave rise to non-stoichiometric $BaFeO_{3-y}$ and $BaCoO_{3-y}$ phases at temperatures and reaction times much lower than those of the ceramic method.

Experimental Section

Materials: Cobalt(II) chloride and malonic acid were purchased from Fluka, iron(II) chloride was purchased from Aldrich and sodium carbonate from Merck. They were all used without further purification.

Physical Measurements: Microanalyses were performed with a LECO CHNS-932 elemental analyser. Analytical measurements were carried out on an ARL 3410+ICP with Minitorch equipment. The powder X-ray diffraction (XRD) pattern was taken using a Philips X′pert diffractometer equipped with graphite-monochromated Cu-$K\alpha_1$ radiation. Data were collected by scanning in the range $5 < 2\theta < 70°$ with increments of 0.02° (2θ). Thermogravimetric measurements were performed on a Perkin−Elmer System-7 DSC-TGA instrument. Crucibles containing 20 mg of sample were heated at 5 °C·min^{-1} under dry nitrogen and air atmospheres. IR spectra (400−4000 cm^{-1}) were recorded on a MATTSON FTIR 1000 spectrophotometer with samples prepared as KBr pellets. Diffuse reflectance spectra were carried out on a CARY 2415 spectrometer in the range 5000−45000 cm^{-1}. Magnetic susceptibility measurements of powdered samples were carried out in the 1.8−300 K temperature range using a Quantum Design MPMS-7 Squid magnetometer. The magnetic measurements were performed at magnetic fields between 0 and 7 T.

Preparation of the Metallo-organic Precursors: To a solution of 2.5 mmol of disodium malonate, previously formed from 2.5 mmol (0.2601 g) of malonic acid neutralised with 2.5 mmol (0.7419 g) of sodium carbonate, 1 mmol of the corresponding transition metal salt was added. The mixture was stirred for 30 minutes and 1 mmol of barium chloride was added. Polycrystalline powders of the two phases were obtained in a few seconds. They were then stirred for 1−2 hours until complete precipitation was attained. For the iron compound, a closed system with a nitrogen atmosphere was needed to prevent oxidation. The powders obtained, white and light pink for the BaFe and the BaCo complexes respectively, were filtered and washed with ethanol/water followed by diethyl ether. Elemental analysis together with Inductively Coupled Plasma measurements were consistent with the following stoichiometries: $BaFeC_6H_{12}O_{12}$ and $BaCoC_6H_{12}O_{12}$. $BaFeC_6H_{12}O_{12}$: calcd. C 15.35, H 2.58, Fe 11.90, Ba 29.26; found. C 15.56, H 2.91, Fe 12.06, Ba 29.83; $BaCoC_6H_{12}O_{12}$: calcd. C 15.25, H 2.56, Co 12.48, Ba 29.07; found. C 15.10, H 2.11, Co 11.90, Ba 28.90.

Acknowledgments

This work has been carried out with the financial support of the MCYT (MAT, 2001-0064) and the Universidad del País Vasco/Euskal Herriko Unibertsitatea (Project 169.310-13494/2001).

[1] C. Ruiz-Pérez, M. Hernández-Molina, P. Lorenzo-Luis, F. Lloret, J. Cano, M. Julve, *Inorg. Chem.* **2000**, *39*, 3845.
[2] R. P. Scaringe, W. E. Hatfield, D. J. Hodgson, *Inorg. Chem.* **1977**, *16*, 1600.
[3] D. Chattopadhyay, S. K. Chattopadhyay, P. R. Lowe, C. H. Schwalke, S. K. Mazumber, A. Rana, S. Ghosh, *J. Chem. Soc., Dalton Trans.* **1993**, 913.
[4] C. Ruiz-Pérez, J. Sanchiz, M. Hernández-Molina, F. Loret, M. Julve, *Inorg. Chem.* **2000**, *39*, 1363; C. Ruiz-Pérez, J. Sanchiz, M. Hernández-Molina, F. Loret, M. Julve, *Inorg. Chim. Acta* **2000**, *298*, 202.
[5] S. H. Saadeh, K. L. Trojan, J. W. Kampf, W. E. Hatfield, V. L. Peroraro, *Inorg. Chem.* **1993**, *32*, 3034.
[6] Y.-G. Wei, S-W. Zhang, M.-C. Shao, Q. Liu, Y.-Q. Tang, *Polyhedron* **1996**, *15*, 4303.
[7] C. Ruiz-Pérez, M. Hernández-Molina, J. Sanchiz, T. López, F. Lloret, M. Julve, *Inorg. Chim. Acta* **2000**, *298*, 245.
[8] I. Gil de Muro, F. A. Mautner, M. Insausti, L. Lezama, M. I. Arriortua, T. Rojo, *Inorg. Chem.* **1998**, *37*, 3243.
[9] Y. Rodriguez-Martín, C. Ruiz-Pérez, J. Sanchiz, F. Loret, M. Julve, *Inorg. Chim. Acta* **2001**, *318*, 159.
[10] C. N. R. Rao, *Chemical Approaches to the Synthesis of Inorganic Materials*, Wiley, New York, **1994**.
[11] K. Vidyasagar, J. Gopalakrishnan, C. N. R. Rao, *Inorg. Chem.* **1984**, *23*, 1206.
[12] T. Rojo, M. Insausti, M. I. Arriortua, E. Hernández, J. Zubillaga, *Thermochim Acta* **1992**, *195*, 95.
[13] M. Insausti, R. Cortés, M. I. Arriortua, T. Rojo, E. Hernández, *Solid State Ionics* **1993**, *63*, 351.
[14] J. García-Jaca, M. Insausti, J. L. Pizarro, R. Cortés, M. I. Arriortua, T. Rojo, *Polyhedron* **1993**, *13*, 357.
[15] A. Bolivar, M. Insausti, L. Lorente, J. L. Pizarro, M. I. Arriortua, T. Rojo, *J. Mater. Chem.* **1997**, *7*, 2259.
[16] M. Insausti, I. Gil de Muro, L. Lorente, T. Rojo, E. H. Bocanegra, M. I. Arriortua, *Thermochim. Acta* **1996**, *287*, 81.

[17] I. Gil de Muro, M. Insausti, L. Lezama, J. L. Pizarro, M. I. Arriortua, T. Rojo, *Eur. J. Inorg. Chem.* **1999**, 935.
[18] I. Gil de Muro, M. Insausti, L. Lezama, M. K. Urtiaga, M. I. Arriortua, T. Rojo, *J. Chem. Soc., Dalton Trans.* **2000**, 3360.
[19] J. Rodríguez-Carvajal, *Physica B* **1993**, *192*, 55.
[20] E. Escrivá, A. Fuertes, J. V. Folgado, E. Martínez-Tamayo, A. Beltrán-Porter, D. Beltrán-Porter, *Thermochim. Acta* **1986**, *104*, 223.
[21] Powder Diffraction File, Card No. 23−1024. Joint Committee on Powder Diffraction Standars, Swarthmore PA, **1995**.
[22] Powder Diffraction File, Card No. 10−245. Joint Committee on Powder Diffraction Standars, Swarthmore PA, **1995**.
[23] K. Nakamoto, *Infrared Spectra of Inorganic and Coordination Compounds*, 5th ed., John Wiley & Sons, New York, **1987**.
[24] A. B. P. Lever, *Inorganic Electronic Spectroscopy*, 2nd ed., Elsevier, New York, **1986**.
[25] G. S. Rushbrooke, P. Wood, *J. Mol. Phys.* **1963**, *6*, 409.
Received February 10, 2003

